This article was downloaded by: [Giorgio Pastore]
On: 09 July 2015, At: 13:57
Publisher: Taylor & Francis
Informa Ltd Registered in England and Wales Registered Number: 1072954 Registered office: 5 Howick Place, London, SW1P 1WG

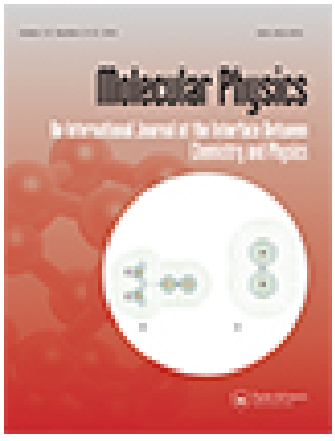

Molecular Physics: An International Journal at the Interface Between Chemistry and Physics
Publication details, including instructions for authors and subscription information:
http://www.tandfonline.com/loi/tmph20

Wertheim perturbation theory: thermodynamics and structure of patchy colloids

Riccardo Fantoni[a] & Giorgio Pastore[b]
[a] Dipartimento di Scienze Molecolari e Nanosistemi, Università Ca' Foscari Venezia, Venezia, Italy
[b] Dipartimento di Fisica, Università di Trieste, Trieste, Italy
Published online: 09 Jul 2015.

Click for updates

To cite this article: Riccardo Fantoni & Giorgio Pastore (2015): Wertheim perturbation theory: thermodynamics and structure of patchy colloids, Molecular Physics: An International Journal at the Interface Between Chemistry and Physics, DOI: 10.1080/00268976.2015.1061150

To link to this article: http://dx.doi.org/10.1080/00268976.2015.1061150

PLEASE SCROLL DOWN FOR ARTICLE

Taylor & Francis makes every effort to ensure the accuracy of all the information (the "Content") contained in the publications on our platform. However, Taylor & Francis, our agents, and our licensors make no representations or warranties whatsoever as to the accuracy, completeness, or suitability for any purpose of the Content. Any opinions and views expressed in this publication are the opinions and views of the authors, and are not the views of or endorsed by Taylor & Francis. The accuracy of the Content should not be relied upon and should be independently verified with primary sources of information. Taylor and Francis shall not be liable for any losses, actions, claims, proceedings, demands, costs, expenses, damages, and other liabilities whatsoever or howsoever caused arising directly or indirectly in connection with, in relation to or arising out of the use of the Content.

This article may be used for research, teaching, and private study purposes. Any substantial or systematic reproduction, redistribution, reselling, loan, sub-licensing, systematic supply, or distribution in any form to anyone is expressly forbidden. Terms & Conditions of access and use can be found at http://www.tandfonline.com/page/terms-and-conditions

Molecular Physics, 2015
http://dx.doi.org/10.1080/00268976.2015.1061150

Taylor & Francis
Taylor & Francis Group

SPECIAL ISSUE IN HONOUR OF JEAN-PIERRE HANSEN

Wertheim perturbation theory: thermodynamics and structure of patchy colloids

Riccardo Fantoni[a] and Giorgio Pastore[b,*]

[a]*Dipartimento di Scienze Molecolari e Nanosistemi, Università Ca' Foscari Venezia, Venezia, Italy;* [b]*Dipartimento di Fisica, Università di Trieste, Trieste, Italy*

(*Received 30 January 2015; accepted 25 May 2015*)

We critically discuss the application of the Wertheim's theory to classes of complex associating fluids that can be today engineered in the laboratory as patchy colloids and to the prediction of their peculiar gas–liquid phase diagrams. Our systematic study, stemming from perturbative version of the theory, allows us to show that, even at the simplest level of approximation for the inter-cluster correlations, the theory is still able to provide a consistent and stable picture of the behaviour of interesting models of self-assembling colloidal suspension. We extend the analysis of a few cases of patchy systems recently introduced in the literature. In particular, we discuss for the first time in detail the consistency of the structural description underlying the perturbative approach and we are able to prove a consistency relationship between the valence as obtained from thermodynamics and from the structure for the one-site case. A simple analytical expression for the structure factor is proposed.

Keywords: colloidal suspensions; Wertheim thermodynamic perturbation theory; associating fluids; structure of fluids

Downloaded by [Giorgio Pastore] at 13:57 09 July 2015

1. Introduction

Recently, there have been interesting developments of techniques for the synthesis of new colloidal patchy particles in the laboratory [1], including seeded growth, swelling, and phase separation. Whereas in the laboratory, relatively less work has been done on the thermodynamic characterisation of self-assembly of these particles, from a theoretical point of view, or in recent computer experiments, these kind of associating fluids [2] and their clustering and phase behaviour are actively studied [3–9].

In principle, statistical mechanics should be able to describe all equilibrium phases. However, the strong and confined attractions responsible of association call for a more clever approach than brute force. In particular, it has been found useful to describe an associating fluid as one where there are n_c species of clusters made of a number i of particles, denoted i-mers. Many definitions of cluster are possible [10–15] either of a geometric nature or of a topological one, depending on the spatial arrangement of the bonded particles. If we measure the concentrations of the i-mers in an associating fluid, we will find that they are functions of the thermodynamic state: for one-component systems, the temperature T and the density ρ of the fluid. Then, special statistical mechanics approaches have been developed to obtain such information and phase diagrams from models of interactions.

In our previous work [2], we compared two theories for cluster equilibria, the Wertheim association theory [16–19] and the Bjerrum-Tani-Henderson theory [20–26] and we showed that for $n_c = 2$, the two approaches coincide when inter-cluster correlation are ignored, i.e. the system behaves as an ideal gas of clusters. Nonetheless, the simple and elegant perturbation theory described in Wertheim's work is able, unlike the one of Bjerrum-Tani-Henderson, to describe the case of $n_c \to \infty$ fluids. Due to this fact, Wertheim theory is able to describe the liquid phase, thus giving access to the study of liquid–gas coexistence in a coherent way, while the Bjerrum-Tani-Henderson one is not. The first order in the Wertheim perturbation theory approximation is a simple but very useful tool. At high temperature, the associating fluid reduces to the 'reference' fluid that can also be considered as the one obtained from the associating fluid switching off all attractions. However, in its original form, the theory is only applicable when some 'steric incompatibility' conditions are fulfilled by the associating fluid: a single bond per site, no more than one bond between any two particles, and no closed loop, or ring, of bonds.

Patchy colloids are systems of current experimental and theoretical [1,27] interest. Simple models for their interactions, for example fluids of hard-spheres (HSs) decorated with attractive sites distributed on their surface, are well suited for application of Wertheim theory. For particles with M identical bonding sites, Bianchi *et al.* [3–5] discovered the 'empty liquid' scenario as M approaches two, i.e. when the clusters allowed in the fluid are just the 'chains'. Even more rich phenomenology is found when there are

* Corresponding author. Email: pastore@ts.infn.it

© 2015 Taylor & Francis

Downloaded by [Giorgio Pastore] at 13:57 09 July 2015

sites of two different kinds [6,7] and 'junctions' formation becomes possible. Such structures become responsible for a re-entrance of the liquid branch of the binodal, and for 'rings' formation [8,9]. Moreover, extending Wertheim theory beyond its steric incompatibility conditions, the rings formation has been found to be responsible for a re-entrance also in the gas branch and the appearance of a second lower critical point (recently appeared studies which further extend Wertheim theory to allow also for doubly bonded sites [28–30]). From all these studies emerged how Wertheim theory has very good semi-quantitative agreement with exact Monte Carlo (MC) simulations, when applied to these one-component patchy particle fluids (especially so at the level of the clusters concentrations behavior). Far from being a purely theoretical speculation, these fluids can be engineered in the laboratory [1] from patchy colloids.

In the present work, while critically reviewing such theoretical results, in particular elucidating the role of the accuracy of inter cluster correlations, we will discuss the solution of the Wertheim theory applied to HSs with M identical bonding sites and with sites of two different kinds. Our analysis is intended to be as simple and systematic as possible while re-analysing the many works found in the literature on various particular highly idealised associating colloidal suspension models. This will allow us to treat the ring forming systems of Rovigatti *et al.* [8,9] fully analytically as freely jointed chains. We show that also the results in Ref. [31], extending Russo *et al.* [6,7] results to take into account the 'X-junctions' formation, and in particular, the existence of characteristic 'R'-shaped spinodals, are largely independent on the choice of the reference system correlations. Moreover, we find the indication of a gas–liquid coexistence with a critical point at extremely low densities and temperatures at $r < 1/3$, with r the ratio between the gain in energy between the bond of two unlike sites and the one between two like sites.

We also study in detail the relationship between structural and thermodynamic information within Wertheim theory, and in particular between the effective valence as obtained from the thermodynamics and from the structure.

The paper is organised as follows: in Section 2, we introduce the thermodynamic quantities we will take under consideration in the rest of the work; in Section 3, we will review Wertheim association theory in the light of the present work needs, the problem of identical attractive site (Section 3.1.2), and the problem of attractive sites of two different kinds (Section 3.1.3); in Section 3.2, we introduce the problem of the gas–liquid coexistence; in Section 3.3, we comment on the relevance of the pair-potential microscopic level of description; and in Section 4, we systematically re-analyse many results obtained applying Wertheim theory to specific fluids with identical sites (Section 4.1) and sites of two different kinds (Section 4.2). We show, in a systematic way, that all the results present in the literature are structurally stable with respect to changes in the reference system accuracy; in Section 6, we determine a simple analytical expression for the radial distribution function which we then use to calculate the valence; in Section 7, we determine a simple analytical expression for the structure factor; and Section 8 is for final remarks.

2. Thermodynamics

Consider a one-component fluid of N associating HS particles in a volume V at an absolute temperature $T = 1/\beta k_B$ with k_B Boltzmann constant.

The Helmholtz free energy A of a HS associating fluid can be written as a sum of separate contributions [32]

$$A = A_0 + A_{mf} + A_{\text{bond}}, \tag{1}$$

where A_0 is the free energy of a HS fluid at a density $\rho = N/V$, A_{mf} is the mean-field contribution due to the dispersion forces, and A_{bond} is the change in the free energy due to association. We will generally use the notation $a(\rho, T) = a = A/N$ for the free energy per particle.

The HS free energy per particle in excess of the ideal gas one is accurately given by the Carnahan and Starling expression [33]

$$\beta a_0^{ex} = \frac{4\eta - 3\eta^2}{(1-\eta)^2}, \tag{2}$$

where $\eta = (\pi/6)\rho\sigma^3$ is the packing fraction of the HSs of diameter σ. So that adding the ideal gas contribution $\beta a_{id} = \ln(\rho\Lambda^3/e)$, with Λ the de Broglie thermal wavelength, we obtain $a_0 = a_{id} + a_0^{ex}$.

The mean-field contribution has the van der Waals form

$$\beta a_{mf} = -\frac{\epsilon_{mf}\rho}{k_B T}, \tag{3}$$

where the constant ϵ_{mf} is the measure of the strength of the mean-field attractions. The addition of this contribution to A_0 is essential to have a gas–liquid coexistence.

From a microscopic point of view, one can see, for example, the mean-field contribution as arising from the first order in β in a high-temperature expansion of a thermodynamic perturbation theory treatment of the square-well (SW) fluid, with the HS taken as the reference system. So, the free energy of the corresponding associating fluid will be given by $A = A_{SW} + A_{\text{bond}}$. But, as we will see in Section 4, one can have gas–liquid coexistence with just $A = A_0 + A_{\text{bond}}$ for a properly chosen A_{bond}.

We can define a unit of length, $\mathcal{S}$, and a unit of energy, $\mathcal{E}$, so that we can introduce a reduced density, $\rho^* = \rho\mathcal{S}^3$, and a reduced temperature, $T^* = k_B T/\mathcal{E}$.

The association contribution A_{bond} will be discussed in the next section.

Downloaded by [Giorgio Pastore] at 13:57 09 July 2015

3. Associating fluids

We recall here the main result of Wertheim association theory [16–19]. We write the bond free energy per particle $a_{\rm bond}$ such that the full free energy per particle of the associating fluid can be written as $a = a_0 + a_{\rm bond}$, where a_0 is the contribution of the reference fluid, the one obtained from the associating fluid setting to zero all the bonding attractions. We discuss the importance of the choice of a proper pair-potential for the fulfillment of the steric incompatibility conditions in the microscopic description of the fluid. And we discuss the problem of the determination of the gas–liquid coexistence line (the binodal) in our one-component fluid.

3.1. Wertheim statistical thermodynamic theory

In Wertheim theory [16–19], one assumes that each HS of the one-component fluid is decorated with a set Γ of M attractive sites. Under the assumptions of: (1) a single bond per site, (2) no more than one bond between any two particles, and (3) no closed loop, or ring, of bonds, one can write in a first-order thermodynamic perturbation theory framework, valid at reasonably high temperatures,

$$\beta a^W_{\rm bond} = \sum_{\alpha\in\Gamma}\left(\ln x_\alpha - \frac{x_\alpha}{2}\right) + \frac{M}{2}, \tag{4}$$

where $x_\alpha = N_\alpha/N$ is the fraction of sites α that are not bonded. We will also introduce the symbol x_i to denote the concentration of clusters made of a number i of particles. We will always use a Greek index to denote a specific site. We can solve for the x_α from the 'law of mass action'

$$x_\alpha = \frac{1}{1+\rho\sum_{\beta\in\Gamma} x_\beta \Delta_{\alpha\beta}}, \quad \alpha\in\Gamma \tag{5}$$

where the probability to form a bond, once the available sites of the two particles are chosen, is given by $\rho\Delta_{\alpha\beta} = \rho\Delta_{\beta\alpha}$ and approximated as

$$\Delta_{\alpha\beta} = \int g_0(r_{12})\langle f_{\alpha\beta}(12)\rangle_{\Omega_1,\Omega_2} d\mathbf{r}_{12}. \tag{6}$$

Here, g_0 is the radial distribution function of the reference system, $f_{\alpha\beta}$ is the Mayer function between site α on particle 1 and site β on particle 2 (see Section 3.3), and $\langle\ldots\rangle_{\Omega_1,\Omega_2}$ denotes an angular average over all orientations of particles 1 and 2 at a fixed relative distance r_{12}. Equation (5) should be solved for the real physically relevant solution such that $\lim_{\rho\to 0} x_\alpha = 1$. Even if we cannot exclude the possibility of having multiple solutions satisfying to this condition, we never encountered such a case in the present work. Clearly, we cannot assign any physical value to the branches with $x_\alpha \notin [0, 1]$.

At high temperatures $\Delta_{\alpha\beta} \to 0$ and $x_\alpha \to 1$, which means we have complete dissociation. At low temperatures (Wertheim theory is a high-temperature expansion but here we just mean the formal low T limit of the first-order Wertheim results) $\Delta_{\alpha\beta} \to \infty$ and $x_\alpha \to 0$, which means that we have complete association.

The number of attractive sites controls the physical behaviour. Models with one site allow only dimerisation. The presence of two sites permits the formation of chain and ring polymers. Additional sites allow formation of branched polymers and amorphous systems.

3.1.1. One attractive site

The case of a single attractive site was carefully considered in our previous work [2] where a comparison between the Wertheim theory and the Bjerrum-Tani-Henderson theory [20–26] was made.

3.1.2. Identical attractive sites

Another simple case we can consider in Wertheim theory is the one with M identical attractive sites of kind A (we will always use a capital letter to denote a site kind). Now, the law of mass action for $x = x_A$ (the fraction of unbonded specific sites of kind A) is solved by

$$x = \frac{2}{1+\sqrt{1+4M\rho\Delta}}, \tag{7}$$

with $\Delta = \Delta_{AA}$.

The free energy contribution due to association is now given by

$$\beta a^W_{\rm bond} = M(\ln x - x/2) + M/2. \tag{8}$$

In this case, $x_1 = x^M$.

3.1.3. Attractive sites of two kinds

A more complex case in Wertheim theory is the one with M_A identical attractive sites of kind A and M_B identical attractive sites of kind B. Now, the law of mass action reduces to the following system of two coupled quadratic equations

$$x_A + M_A\rho\Delta_{AA}x_A^2 + M_B\rho\Delta_{AB}x_Ax_B = 1, \tag{9}$$

$$x_B + M_B\rho\Delta_{BB}x_B^2 + M_A\rho\Delta_{AB}x_Ax_B = 1, \tag{10}$$

which admits in general a set of four different solutions for (x_A, x_B) from which it is necessary to single out the physically relevant one. In the event that there is no attraction between a site of kind A and a site of kind B, then $\Delta_{AB} = 0$ and the system simplifies to

$$x_A = \frac{2}{1+\sqrt{1+4M_A\rho\Delta_{AA}}}, \tag{11}$$

$$x_B = \frac{2}{1+\sqrt{1+4M_B\rho\Delta_{BB}}}. \tag{12}$$

In the event that there is no attraction between sites of the same kind, it simplifies to

$$x_A = 2/\{1+(M_B-M_A)\rho\Delta_{AB} + \sqrt{[1+(M_B-M_A)\rho\Delta_{AB}]^2+4M_A\rho\Delta_{AB}}\}, \tag{13}$$

and x_B obtained exchanging $A\leftrightarrow B$ in the equation above.

The free energy contribution due to association is now given by

$$\beta a^W_{\rm bond} = M_A(\ln x_A - x_A/2) + M_A/2 + M_B(\ln x_B - x_B/2) + M_B/2. \tag{14}$$

In this case, $x_1 = x_A^{M_A}x_B^{M_B}$.

3.2. *The gas–liquid coexistence*

In order to determine the gas–liquid coexistence line (the binodal), one needs to find the compressibility factor $z = \beta p/\rho$, with p the pressure, and the chemical potential μ of the associating fluid according to the thermodynamic relations

$$z(\rho,T) = \rho\left(\frac{\partial\beta a}{\partial\rho}\right)_{T,N}, \tag{15}$$

$$\beta\mu(\rho,T) = \left(\frac{\partial\beta a\rho}{\partial\rho}\right)_{T,V} = z+\beta a. \tag{16}$$

The coexistence line is then given by the Gibbs equilibrium condition of equality of the pressures and chemical potentials of the two phases

$$\rho_g z(\rho_g,T) = \rho_l z(\rho_l,T), \tag{17}$$

$$\beta\mu(\rho_g,T) = \beta\mu(\rho_l,T), \tag{18}$$

from which one can find the coexistence density of the gas $\rho_g(T)$ and of the liquid $\rho_l(T)$ phases.

The critical point (ρ_c, T_c) is determined by solving the following system of equations

$$\left.\frac{\partial z\rho}{\partial\rho}\right|_{\rho_c,T_c} = 0, \tag{19}$$

$$\left.\frac{\partial^2 z\rho}{\partial\rho^2}\right|_{\rho_c,T_c} = 0. \tag{20}$$

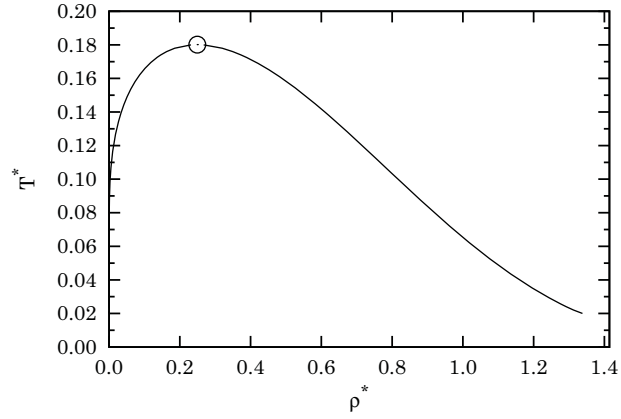

Figure 1. Gas–liquid binodal for the HS plus the van der Waals mean-field term. The circle is the critical point at $\rho_c^* \approx 0.249129$, $T_c^* \approx 0.180155$, and $z_c \approx 0.358956$ [34].

3.2.1. *The mean-field case*

For the HS fluid in the presence of just a van der Waals mean-field free energy contribution, described by Equation (1) without the last association term, the thermodynamics is parameter free. We take the diameter of the spheres σ as the unit of length (so that $\rho^* \in [0,\sqrt{2}]$ with $\sqrt{2}$ the close-packing reduced density) and ϵ_{mf} as the unit of energy. Solving the Gibbs equilibrium conditions of Equations (17) and (18), we find the binodal of Figure 1 and from Equations (19) and (20), we find the critical point.

We can see this case as describing a thermodynamic perturbation theory approximation for a SW fluid to first order in β small [35]. MC simulations of the SW fluid are well known to show a gas–liquid binodal with the critical point shifting at lower temperatures and higher densities as the width of the attractive well decreases [36,37].

Recently [38], it was shown through numerical simulation and theoretical approaches that a binodal with two maxima, implying the existence of a low-density liquid and a high-density liquid, can arise solely from an isotropic interaction potential with an attractive part and with two characteristic short-range repulsive distances.

We consider the binodal of Figure 1 as 'standard' in the sense that the gas branch $T_g(\rho)$ is a monotonously increasing function of density and the liquid branch $T_l(\rho)$ a monotonously decreasing function of density. We will see in the next section that using Wertheim association theory, it is possible to obtain non-standard binodals by replacing the mean-field contribution A_{mf} with a proper association contribution $A_{\rm bond}$.

3.3. *Microscopic description: importance of the pair-potential*

The fluid is assumed to be made of particles interacting only through a pair-potential $\phi(12) = \phi(\mathbf{r}_1,\Omega_1,\mathbf{r}_2,\Omega_2)$ where $\mathbf{r}_i$

Downloaded by [Giorgio Pastore] at 13:57 09 July 2015

Downloaded by [Giorgio Pastore] at 13:57 09 July 2015

and Ω_i are the position vector of the centre of particle i and the orientation of particle i, respectively.

To give structure to the fluid, we further assume that the particles have an isotropic hard-core of diameter σ with

$$\phi(12) = \phi_0(r_{12}) + \Phi(12), \tag{21}$$

where $r_{12} = |\mathbf{r}_{12}| = |\mathbf{r}_2 - \mathbf{r}_1|$ is the separation between the two particles 1 and 2 and

$$\phi_0(r) = \begin{cases} +\infty & r \le \sigma \\ 0 & r > \sigma \end{cases}, \tag{22}$$

The anisotropic part $\Phi(12)$ in Wertheim theory is generally chosen as

$$\Phi(12) = \sum_{\alpha\in\Gamma}\sum_{\beta\in\Gamma} \psi_{\alpha\beta}(r_{\alpha\beta}), \tag{23}$$

where

$$\mathbf{r}_{\alpha\beta} = \mathbf{r}_2 + \mathbf{d}_\beta(\Omega_2) - \mathbf{r}_1 - \mathbf{d}_\alpha(\Omega_1), \tag{24}$$

is the vector connecting site α on particle 1 with site β on particle 2. Here, $\mathbf{d}_\alpha$ is the vector from the particle centre to site α with $d_\alpha < \sigma/2$. The site–site interactions $\psi_{\alpha\beta} \le 0$ are assumed to be purely attractive. The Mayer functions introduced in Section 3.1 are then defined as $f_{\alpha\beta}(12) = \exp[-\beta\psi_{\alpha\beta}(r_{\alpha\beta})] - 1$.

Wertheim theory depends on the specific form of the site–site potential only through the quantity $\Delta_{\alpha\beta}$ of Equation (6), as long as the three conditions of a single bond per site, no more than one bond between any two particles, and no closed loop of bonds, are satisfied. A common choice, for example, is a SW form

$$\psi_{\alpha\beta}(r) = \begin{cases} -\epsilon_{\alpha\beta} & r \le d_{\alpha\beta} \\ 0 & r > d_{\alpha\beta} \end{cases}, \tag{25}$$

where $\epsilon_{\alpha\beta} > 0$ are site–site energy scales, the wells depths, and $d_{\alpha\beta}$ are the wells widths. In this case, we must have $d_\alpha + d_\beta > \sigma - d_{\alpha\beta}$, moreover we will have

$$\Delta_{\alpha\beta} = K_{\alpha\beta}(\sigma, d_{\alpha\beta}, \eta)(e^{\beta\epsilon_{\alpha\beta}} - 1). \tag{26}$$

We will also call $\lim_{\rho\to 0} K_{\alpha\beta} = K^0_{\alpha\beta}$ some purely geometric factors. Remember that $\lim_{\rho\to 0} g_0(r) = \Theta(r-\sigma)$ with Θ the Heaviside step function.

Another common choice is the Kern–Frenkel patch–patch pair-potential model [39].

4. Structural stability of Wertheim theory

There has recently been some relevant progress on the study of several complex associating fluids through MC simulations and theoretically through the Wertheim theory outlined above. The comparison between the two approaches shows semi-quantitative agreement, between the exact MC results and the approximated theoretical results, at the level of description of clusters concentrations and of gas–liquid binodal. We will here return on some of the systems studied from Bianchi *et al.* [3–5], Russo *et al.* [6,7], and Rovigatti *et al.* [8,9] from a unified perspective, and concentrating ourselves on the structural stability of the Wertheim theory, i.e. we will show that all the qualitative non-standard features of the phase diagrams at a large extent do not depend on the accuracy of description of the reference system.

4.1. *Identical sites*

The case of HSs with a number M of identical attractive sites in various geometries on the surface of the spherical particle has been studied by Bianchi *et al.* [3–5]. They showed that the properties of the resulting fluid are largely independent from the sites geometry [5]. And the gas–liquid binodal has a liquid branch moving at lower densities as M decreases. In particular, the binodal vanishes for $M \to 2$, a scenario that they called 'empty liquid': the critical temperature $T_c(M)$ and critical density $\rho_c(M)$ are such that $\lim_{M\to 2} T_c = \bar{T}_c > 0$ and $\lim_{M\to 2}\rho_c = 0$. There is then the formation of a homogeneous disordered material at small densities below $\bar{T}_c$, i.e. a stable equilibrium gel. Moreover, in their fluid with $M = 2$, Bianchi *et al.* observed linear 'chains' formation: 'chaining'.

This is quite different from what happens in fluids of Kern and Frenkel patchy HSs varying the patches surface coverages [40]. In Ref. [40], a study of criticality similar to the one of Bianchi was made varying the attractive patch surface coverage χ. As the surface coverage χ vanishes, $\lim_{\chi\to 0} T_c = \lim_{\chi\to 0}\rho_c = 0$ was found in such cases.

Liu *et al.* [35] repeated Bianchi study for a system of SWs, instead of HSs as in the Bianchi case, with a number M of identical attractive sites. In their study, the gas–liquid coexistence remains also for $M \to 0$, as expected in view of the comments of Section 3.2.1.

4.1.1. *Gas–liquid binodal*

With M identical sites of kind A, we have in the site–site interaction $\epsilon_{AA} = \epsilon$ which we take as unit of energy and again we take σ as unit of length.

We now choose $a = a_0 + a_{\text{bond}}$ with the association part given by the Wertheim theory Equation (4) with M identical sites (see Section 3.1.2).

Following Ref. [4], we choose the identical sites distributed on the surface of the spherical particle and

$$d_{AA} = d = \left(\sqrt{5 - 2\sqrt{3}} - 1\right)\sigma/2 \approx 0.120\sigma, \tag{27}$$

which guarantees that each site is engaged at most in one bond. Moreover, we approximate the radial distribution

Downloaded by [Giorgio Pastore] at 13:57 09 July 2015

function of the reference system with its zero density limit taking $\Delta_{AA} = \Delta = K^0[e^{\beta\epsilon} - 1]$ and using, in Equation (26), the following expressions

$$\langle f_{AA}(12)\rangle = (e^{\beta\epsilon} - 1) m_{AA}(r_{12}) \quad r_{12} > \sigma, \tag{28}$$

$$m_{AA}(r) = \begin{cases} \dfrac{(d+\sigma-r)^2(2d-\sigma+r)}{6r\sigma^2} & \sigma < r < \sigma + d \\ 0 & r > \sigma + d \end{cases}, \tag{29}$$

$$\begin{aligned} K^0_{AA} = K^0 &= 4\pi \int_\sigma^{\sigma+d} m_{AA}(r) r^2 dr \\ &= \pi d^4 (15\sigma + 4d)/30\sigma^2 \\ &\approx 0.332 \times 10^{-3} \sigma^3. \end{aligned} \tag{30}$$

In Figure 2, we show the evolution of the gas–liquid binodal as a function of M, the only free parameter in Wertheim thermodynamic perturbation theory. Compared with Figure 4 of Bianchi *et al.* [3], we see how the qualitative behaviour stays the same even if the two figures differ slightly quantitatively due to our further approximation of taking the radial distribution of the reference system equal to one in the range where bonding occurs. This shows how the Wertheim theory is robust in its qualitative phase diagram predictions. The binodal appears to be always a standard one. And, as we can see from the figure, upon approaching $M \to 2$, the coexistence disappears. Bianchi *et al.* [3] called this phenomenon the empty liquid scenario. It in particular tells us that the fluid with $M = 2$, with the two sites chosen at the spherical particle poles in order to avoid the formations of rings (closed loops of bonds), is made only by chains and does not admit a gas–liquid coexistence. The non-integer M cases can be realised through a binary mixture [3,41,42].

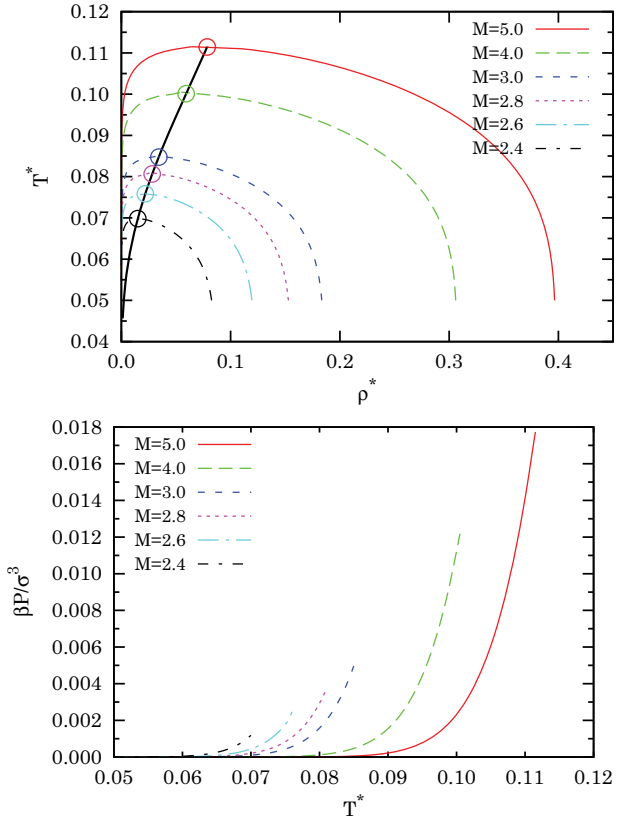

Figure 2. Top panel: evolution of the gas–liquid binodal as a function of M. The continuous thick black line is the locus of the critical points for $M \in]2, 5]$. Bottom panel: pressure–temperature diagram.

From the point of view of Wertheim theory, the reason for this scenario can be explained simply by looking at the low-temperature limit for the bond contribution to the pressure

$$\begin{aligned} \beta p^W_{\text{bond}} = \rho z^W_{\text{bond}} &= \rho^2 \frac{\partial \beta a^W_{\text{bond}}}{\partial \rho} \\ &= -\frac{2M^2\Delta\rho^2}{\left(1 + \sqrt{1 + 4M\Delta\rho}\right)^2} \overset{\Delta\to\infty}{\longrightarrow} -\frac{M}{2}\rho. \end{aligned} \tag{31}$$

From which immediately follows that for $M > 2$, the pressure as a function of density on a low-temperature isotherm shows a van der Waals loop at low densities, which implies the occurrence of a gas–liquid coexistence region.

4.2. *Sites of two kinds*

Tavares *et al.* [43,44] studied the case of HS with three sites, two identical A sites at the poles and a third B one. In addition to chaining, here they observe the formation of 'junctions': 'branching'; rings formation is inhibited in these cases since the A sites at the poles have very small well widths and the B site position is chosen so as to avoid small bond loops, i.e. triangular and square arrangements of bonded particles. Two types of junctions are possible in models where AA bonds are responsible for the chaining: X-shaped junctions, due to BB bonds, and Y-shaped junctions, due to AB bonds. They found that when two of the three interaction strengths vanish simultaneously, there can be no liquid–vapour coexistence. These correspond to the limits of non-interacting linear chains ($\epsilon_{AA} \neq 0$, $\epsilon_{BB} = \epsilon_{AB} = 0$), dimers ($\epsilon_{BB} \neq 0$, $\epsilon_{AA} = \epsilon_{AB} = 0$), and hyperbranched polymers ($\epsilon_{AB} \neq 0$, $\epsilon_{AA} = \epsilon_{BB} = 0$) of Equation (13). They also showed that the phase transition always disappears as $\epsilon_{AA} \to 0$. Moreover, they showed that whereas 'X-junctions' only yield a critical point if their formation is energetically favourable, fluids with 'Y-junctions' will exhibit a critical point, even if forming them raises the energy, provided this increase is below a certain threshold.

Russo *et al.* [6,7] extended Tavares study to the case of two identical small A sites at the poles and nine equispaced identical big B sites on the equator. Killing the interaction

Downloaded by [Giorgio Pastore] at 13:57 09 July 2015

between two B sites ($\epsilon_{BB} = 0$), they observed the formation of chains and Y-junctions (and possibly hyperbranched polymers for $\epsilon_{AB}/\epsilon_{AA}$ large enough) and eventually a re-entrant behaviour of the liquid branch of the gas–liquid binodal pinched at low temperatures.

Rovigatti *et al.* [8,9] extended Russo model selecting an off-pole position of the A sites, thus adding the possibility of 'rings' formation, and observed re-entrance both in the gas and in the liquid branch of the binodal with a second lower critical point where the coexistence curves close itself at low temperatures without the pinch. They needed to relax assumption (3) in Wertheim theory [45–47].

4.2.1. *Gas–liquid binodal*

Russo *et al.* [6] studied the case of sites of two different kinds when the site–site interaction is restricted to $\epsilon_{BB} = 0$ (no X-junctions). Then, choosing as unit of energy ϵ_{AA} and again σ as the unit of length, the Wertheim theory depends on only five parameters: $r = \epsilon_{AB}/\epsilon_{AA} > 0$ and M_A, M_B, K_{AA}, K_{AB}.

We now choose $a = a_0 + a_{\text{bond}}$ with the association part given by the Wertheim theory Equation (4) with sites of two different kinds (see Section 3.1.3). In particular with the condition $\epsilon_{BB} = 0$, Equations (9) and (10) admit just a set of three different solutions for (x_A, x_B) from which it is necessary to single out the real physically relevant one such that $\lim_{\rho \to 0} x_A = \lim_{\rho \to 0} x_B = 1$.

Following Ref. [6], we choose $M_A = 2$, $M_B = 9$ (see Figure 3) and $K^0_{AA} = 1.80 \times 10^{-4}\sigma^3$, $K^0_{AB} = 1.56 \times 10^{-2}\sigma^3$. In order to fulfil the Wertheim condition [(1), of a single bond per site, the small A sites are meant to reside at the particle poles and the big B sites equispaced on the particle equator. The choice of $K^0_{AA} \ll K^0_{AB}$ and the large M_B make branching entropically favourable. We then approximate $\Delta_{AA} = K^0_{AA}(e^{\beta\epsilon_{AA}} - 1)$ and $\Delta_{AB} = K^0_{AB}(e^{\beta\epsilon_{AB}} - 1)$.

In Figure 4, we show the evolution of the gas–liquid binodal as a function of r. Once again, comparing with Figure 3 of Russo *et al.* [6], we observe a complete qualitative agreement, even if in our calculation we further approximated the radial distribution of the reference system equal to one independently of density. We see that for $r < 1/2$, we

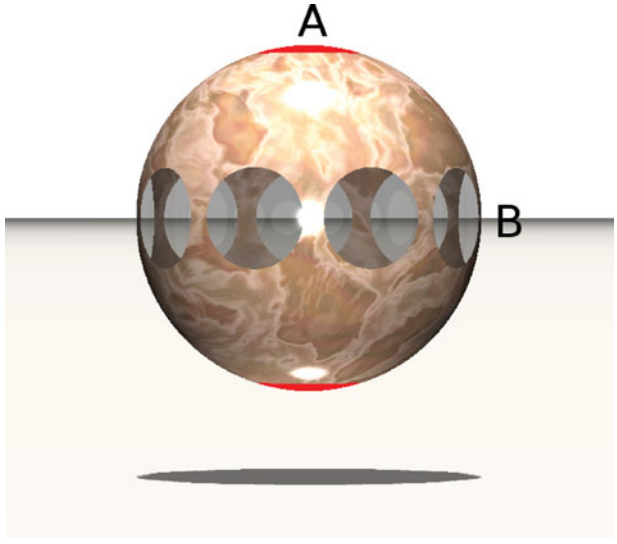

Figure 3. (color online) Pictorial view of a colloidal particle with attractive sites of two different kinds: two A sites on the poles and nine B sites on the equator.

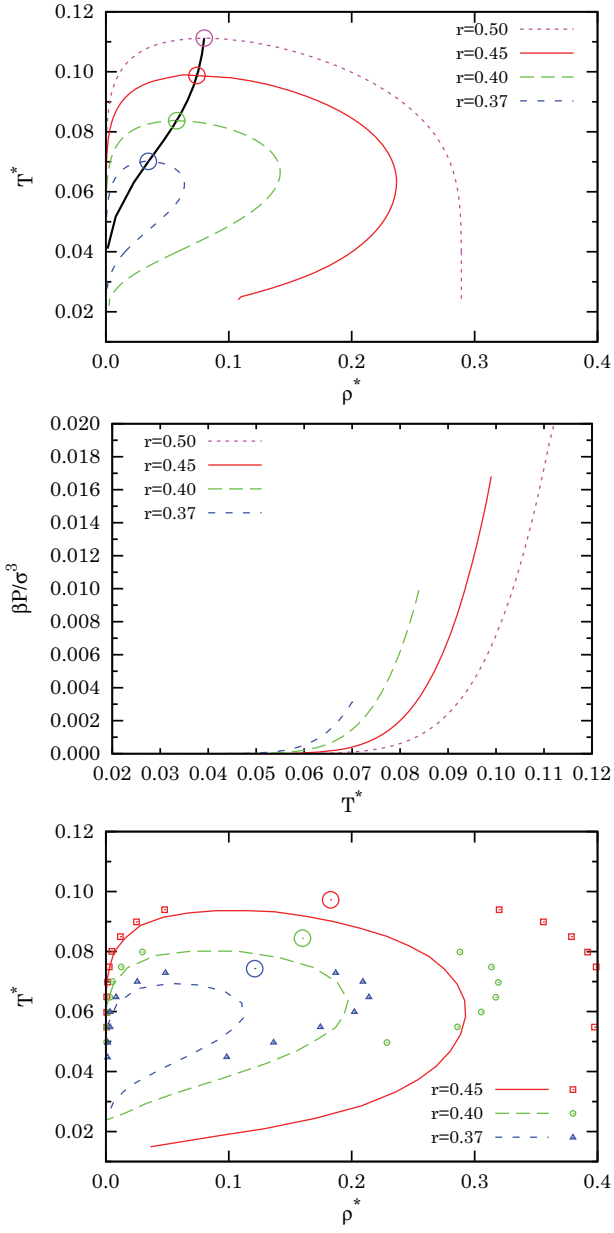

Figure 4. Top panel: evolution of the gas–liquid binodal as a function of r. The continuous thick black line is the locus of the critical points for $r \in]1/3, 1/2]$. Middle panel: pressure–temperature diagram. Bottom panel: binodals of Russo *et al.* [7] Figure 4 as obtained from their analysis (lines) of the Wertheim theory and from their MC simulations (points); the big circles are their predicted critical points.

Downloaded by [Giorgio Pastore] at 13:57 09 July 2015

have a non-standard binodal with a re-entrant liquid branch and a 'pinched' shape evidence that indeed the topological phase separation of Tlusty and Safran [48] is observed. Russo *et al.* [6] were able to provide a qualitative explanation for this behaviour by analysing the energetic of the junction formation process: since the energy cost of forming a chain end is $\epsilon_{\text{chain}} = \epsilon_{AA}/2 > 0$ and the energy cost of forming a Y-junction is $\epsilon_{Y-\text{junction}} = -\epsilon_{AB} + \epsilon_{AA}/2 = \epsilon_{AA}(1/2 - r)$, for $r < 1/2$ we have $\epsilon_{Y-\text{junction}} < 0$, and at low temperatures only chains, which we already saw that do not phase separate, are present.

They are also able to conclude that phase separation occurs only if $r > 1/3$. For $r < 1/3$, the energy cost of forming junctions being too high or, alternatively, the entropy gain being too small to offset the loss of translational entropy of chains in the liquid phase.

This behaviour can be understood by looking at $f(T, \rho; r) = d\beta p/d\rho = d\beta(p_0 + p^W_{\text{bond}})/d\rho$. Differently from Bianchi *et al.* case, now we have $\lim_{\rho\to 0} d\beta p^W_{\text{bond}}/d\rho = 0$. The zeroes of f are two lines in the (ρ, T) plane, one for the minima of the pressure and one for the maxima. The union of the two lines is called the spinodal line for the coexistence. The equal area construction tells us that the binodal line encloses the spinodal line and the two lines are tangent at the critical point. In Figure 5, we show a tridimensional plot of f for $r = 0.36, 2/5, 1/2$ as a function of temperature and density. Clearly, the three different scenarios do not depend on the specific values of K_{AA}, K_{AB}, M_A, M_B which only influence the region in the phase diagram (ρ, T) where we have the van der Waals loop.

The cluster populations for the chain ends, $2x_A$, and Y-junctions, $9(1 - x_B)$, along the binodal were studied in Ref. [6] and are shown in their Figure 4. From Figure 9 of Ref. [7], we see how the mean value of the number of bonds per particle (the valence), $2(1 - x_A) + 9(1 - x_B)$, tends to 2 at low temperatures, i.e. the fluid tends to be formed essentially by chains which, in agreement with Bianchi *et al.* analysis, are unable to sustain the gas–liquid coexistence.

The study of Russo *et al.* differs substantially from the Janus fluid case [22–24,49] where it is found a re-entrant gas branch for the gas–liquid binodal.

Rovigatti *et al.* [9] extended Russo study to take account of rings formation. In this case, the expression for the Wertheim bond free energy per particle of Equation (14) with $M_A = 2$ should be corrected as follows:

$$\beta a^W_{\text{bond}} = \ln\left(y x_B^{M_B}\right) - x_A - \frac{M_B}{2} x_B + 1 + \frac{M_B}{2} - \frac{G_0}{\rho}, \tag{32}$$

where G_n is the nth moment of the rings size distribution

$$G_n = \sum_{i=i_{\min}}^{\infty} i^n W_i (2\rho \Delta_{AA} y)^i, \tag{33}$$

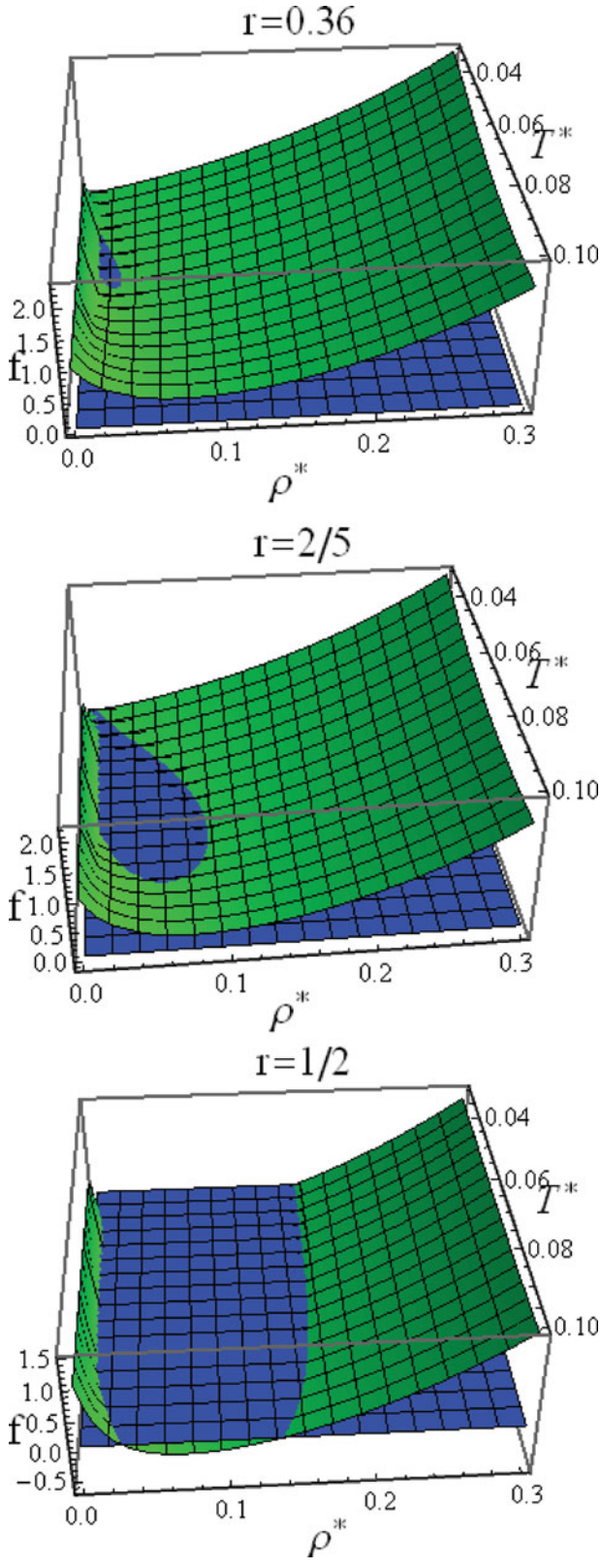

Figure 5. Tridimensional plots of $f(T, \rho; r) = d\beta p/d\rho$ (green surface) for $r = 0.36, 2/5, 1/2$ from top to bottom. Also, shown is the plane $f = 0$ (blue surface). For $r = 1/3$, the two surfaces become tangent at small temperatures and small densities. For $r > 1/2$, the minimum in the pressure moves at larger densities at smaller temperatures.

Downloaded by [Giorgio Pastore] at 13:57 09 July 2015

here $i_{\min}$ is the minimum ring size, y is the fraction of particles with the two A sites unbonded, and W_i is the number of configurations of a ring of size i. Assuming for the rings the freely jointed chain level of description, we can approximate [45]

$$(i+1)W_{i+1} = \frac{i(i-1)}{8\pi} \sum_{j=0}^{l} \frac{(-1)^j}{j!(i-j)!} \left(\frac{i-1-2j}{2}\right)^{i-2}, \tag{34}$$

for l the smallest integer which satisfies $l \geq (i-1)/2 - 1$. Expression (34) is due to Treloar [50] and is the value of the end-to-end distribution function for a freely jointed chain of i links, when the end links are the length of one link apart (the link length is equal to the diameter of a sphere which we take to be our unit of length). For $i \gg 1$, it has the following asymptotic behaviour [50]

$$(i+1)W_{i+1} \approx \left(\frac{3}{2\pi i}\right)^{3/2} e^{-3/2i}, \quad i \gg 1, \tag{35}$$

The laws of mass action of Equations (9) and (10), for $\epsilon_{BB} = 0$, should now be corrected to take into account of the $G_n \neq 0$ as follows:

$$x_A^2 = y(1 - G_1/\rho), \tag{36}$$

$$1 - x_A = M_B \rho \Delta_{AB} x_B x_A + 2\rho \Delta_{AA} x_A^2 + G_1/\rho, \tag{37}$$

$$1 - x_B = 2\rho \Delta_{AB} x_A x_B. \tag{38}$$

Note that solving for x_A Equation (36) and for x_B Equation (38) and substituting into Equation (37), one finds an equation in y only, which always admits just one solution $\bar{y}$ with the properties $0 \leq \bar{y} \leq 1$ and $\lim_{T\to 0} \bar{y} = 0$.

In Figure 6, we show our theoretical numerical results for the gas–liquid binodal of the ring forming fluid. A comparison with Figure 1 of Rovigatti *et al.* [9] shows again a good qualitative agreement between the two calculations. In our calculation, we retained the first 50 terms in the convergent series of Equation (33) and chose $M_B = 9$ and Δ_{AA}, Δ_{AB} as before. As we can see, the rings formation is responsible for the re-entrance in both the gas and liquid branches of the binodal and for the appearance of a second lower critical point. At $r = 0.37$, we could not find a coexistence line, leaving a system for which self-assembly is the only mechanism for aggregation.

In particular, upon approaching the upper critical point, at $T = T_c^u$, if we make a reversible transformation going from the liquid phase to the vapour phase on an isotherm, at $T < T_c^u$, we will have, as usual

$$\Delta S = \int \frac{\delta Q}{T} = \frac{\lambda_v m}{T} > 0, \tag{39}$$

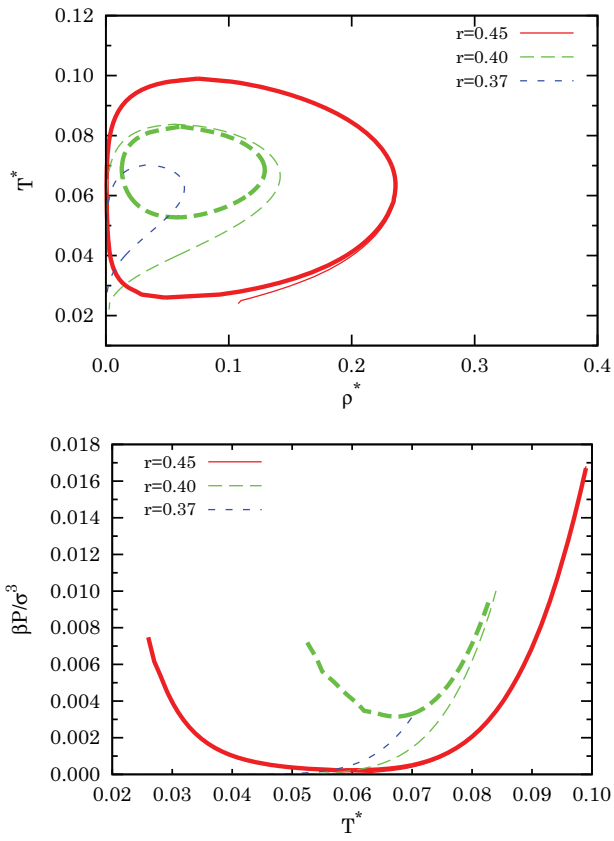

Figure 6. Top panel: evolution of the gas–liquid binodal as a function of r. The thin lines are the binodals of Figure 4. The thick lines are the results obtained for the rings forming fluid. Bottom panel: pressure–temperature diagram.

with ΔS the change in entropy $S = -(\partial A/\partial T)_{N,V}$, δQ the infinitesimal heat exchanges along the path of the transformation, λ_v the 'latent' heat of vaporisation, and m the mass of the fluid. Whereas Rovigatti *et al.* [9] show that upon approaching the lower critical point, at $T = T_c^l$, in the same transformation at $T > T_c^l$, one finds

$$\int \frac{\delta Q}{T} = \frac{\lambda_v m}{T} = \Delta S < 0, \tag{40}$$

so that the 'latent' heat of vaporisation changes sign as T varies from T_c^u to T_c^l. This can be seen directly from our pressure–temperature diagram of Figure 6 using the Clapeyron–Causius formula [51].

Rovigatti analysis neglects the rings with AB bonds. We think that their inclusions may have dramatic effects on the phase diagram.

4.2.2. *A possible extension*

It is possible to extend Russo *et al.* [6,7] results allowing for the $\epsilon_{BB} \neq 0$ condition, responsible for the X-junctions formation [31]. The analysis for just three sites, two of kind

Downloaded by [Giorgio Pastore] at 13:57 09 July 2015

A and one of kind B, can be found in Refs. [43,44] were, interestingly enough, it is found the disappearance of criticality as $\epsilon_{AA} \to 0$. In our extension, we can introduce an additional parameter $s = \epsilon_{BB}/\epsilon_{AA} > 0$. One immediately verifies that the law of mass action of Equations (9) and (10) admits now four solutions (x_A, x_B) from which one has to determine the physical one such that $x_A, x_B \in [0, 1]$ and $\lim_{\rho \to 0} x_A = \lim_{\rho \to 0} x_B = 1$. Clearly, in the limit $r \to 0$, the problem is similar to the one of Bianchi *et al.* [3] (compare Equations (11) and (12) and Equation (7)) and in the limit $s \to 0$, we fall back to Russo *et al.* [6,7] case. We are interested in the non-trivial case: $\Delta_{AA} \neq \Delta_{BB}$ or $M_A \neq M_B$. We will choose for M_A, M_B, K^0_{AA}, and K^0_{AB}, the same values of the Russo's case of Section 4.2.1. Moreover, we will choose $K^0_{BB} = K^0_{AA}$. Again, one has $\lim_{\rho \to 0} d\beta p^W_{\text{bond}}/d\rho = 0$. For s small, we are still able to see the re-entrant liquid scenario contrary to the predictions of Ref. [44]. In other words, we are able to observe a re-entrant liquid branch even in the presence of X-junctions in the fluid, as long as the energy cost for their formation, $\epsilon_{X-\text{junction}} = \epsilon_{AA}(1 - s)$, is positive and big enough. This is shown in Figure 7. The figure also shows how an 'R'-shaped spinodal is possible in these cases with a majority of Y-junctions in correspondence of the coexistence region at high temperature, a majority of X-junctions in correspondence of the coexistence region at low temperature, and a majority of chains in between in correspondence of the bottleneck in the 'R', in agreement with the study of Tavares *et al.* [31]. Moreover, we find gas–liquid coexistence also for $r < 1/3$ as long as s is large enough. This is shown in Figure 8 from which it is also apparent the existence of a gas–liquid coexistence with a critical point at extremely low densities and temperatures, unpredicted by the study of Tavares *et al.* [31]. As a matter of fact, the critical temperature can be made small at will by a proper choice of the control parameters s; the spinodal being essentially independent from r.

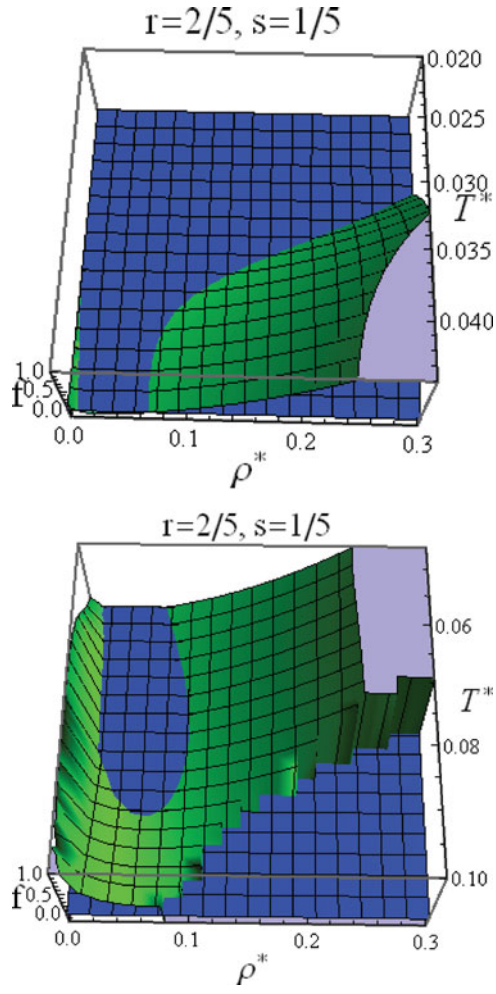

Figure 7. Tridimensional plots of $f(T, \rho; r, s) = d\beta p/d\rho$ (green surface) and of the plane $f = 0$ (blue surface) for $(r, s) = (2/5, 1/5)$. We show two plots one at high temperature and one at low temperature because the (x_A, x_B) physical solution determination changes in the two regions of the phase diagram. The negative f in the high temperature and high density corner of the lowest plot is due to another change in the physical solution determination.

5. Break-down of the theory

Apart from the necessity to fulfil the steric incompatibility conditions, the Wertheim theory will break-down in the following cases:

5.1. *Low temperature limit*

Both the Wertheim theory and the canonical MC simulation break-down at low temperatures. The Wertheim theory is a high-temperature perturbation theory. The first-order version that we have been using until now clearly breaks-down at low temperature when from the mass action law (5) follows that $x_\alpha \to 0$ which in turn produces an undefined bond free energy (4). Also, the usual MC simulation will break-down at very low temperatures. In fact, imagine we have to break a bond with a single particle move. Then, the total energy difference between the final configuration and the initial one would be ϵ and we would need around $1/e^{-\beta\epsilon}$ single particle moves. So, at low temperatures, we would need a very long simulation in order to fully explore configuration space. Depending from the computational resources at one disposal, the range of inaccessible temperatures, before the solidification at zero temperature where the fluid chooses spontaneously the minimum potential energy configuration, may vary. Even if it is possible that patchy fluids, with short-ranged and tunable pair-interactions and with limited valence, will not crystallise at zero temperature [52] remaining a liquid in that limit.

5.2. *Infinite number of attractive sites*

The Wertheim theory will not be applicable anymore to particles decorated with too many attractive sites. In the

Downloaded by [Giorgio Pastore] at 13:57 09 July 2015

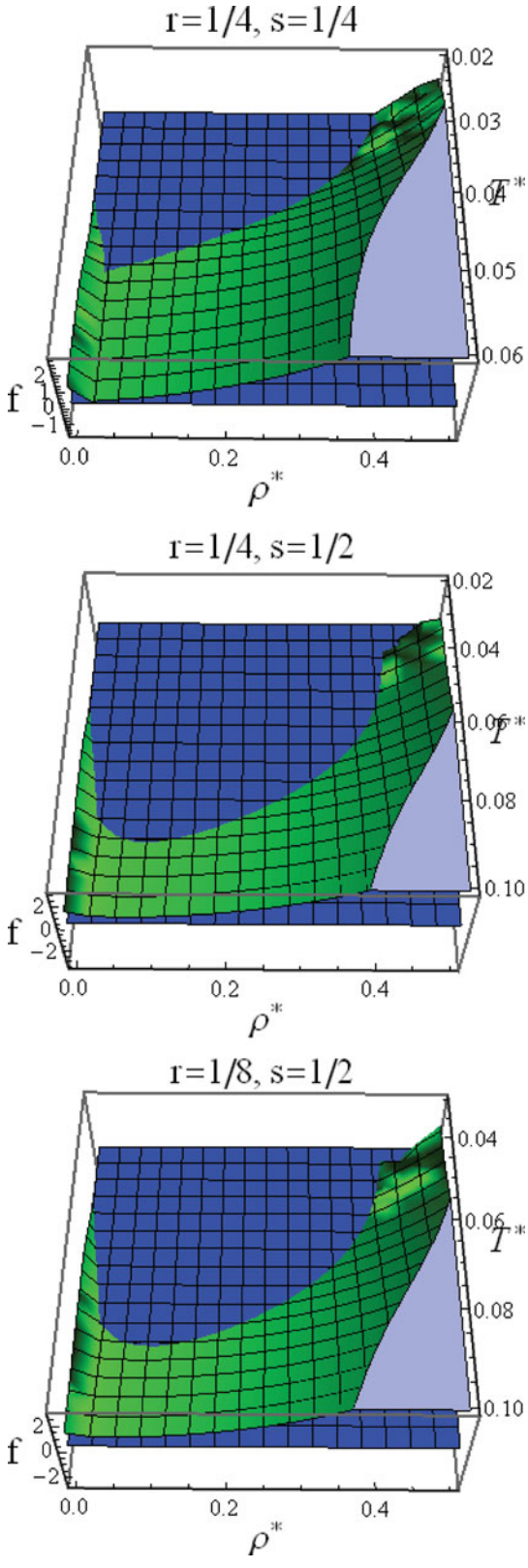

Figure 8. Tridimensional plots of $f(T, \rho; r, s) = d\beta p/d\rho$ (green surface) for $(r, s) = (1/4, 1/4), (1/4, 1/2), (1/8, 1/2)$. Also shown is the plane $f = 0$ (blue surface). As we can see, the spinodals of the two cases $(r, s) = (1/4, 1/2), (1/8, 1/2)$ look essentially the same.

limit of an infinite number of sites uniformly distributed over the particle surface, one recovers the SW fluid or the mean-field solution of Section 3.2.1.

6. The radial distribution function

Using the fact that the angular average of the functional derivative of the free energy per particle respect to the angle dependent pair-potential is equal to $\rho/2V$ times the radial distribution function of colloid centres, we can write

$$g(r) = g_0(r) + \frac{2V}{\rho}\left\langle \frac{\delta a^W_{\text{bond}}}{\delta\phi(1,2)}\right\rangle \tag{41}$$

$$= g_0(r) + \frac{2}{\rho}\frac{1}{4\pi r^2}\sum_{\gamma\in\Gamma}\left(\frac{1}{x_\gamma} - \frac{1}{2}\right) \times \left\langle \frac{\delta x_\gamma}{\delta\left[\sum_{\alpha,\beta\in\Gamma}\beta\psi_{\alpha\beta}(r_{\alpha\beta})\right]}\right\rangle, \tag{42}$$

where we denote with $\langle \ldots \rangle$ the orientational average, and in the second equality, we used Equations (4) and (21).

To make some progress, we use the following property

$$\left\langle \frac{\delta\langle f_{\alpha\beta}\rangle}{\delta\beta\psi_{\alpha\beta}}\right\rangle = -m_{\alpha\beta}(r)e^{\beta\epsilon_{\alpha\beta}} = -m_{\alpha\beta}(r) - \langle f_{\alpha\beta}\rangle \tag{43}$$

where in the last equality, we used Equations (28) and (29). From Equation (6) follows

$$\delta\Delta_{\alpha\beta}/\delta\langle f_{\alpha\beta}(12)\rangle = 4\pi r_{12}^2 g_0(r_{12}) I_{\alpha\beta}(r_{12}), \tag{44}$$

where $I_{\alpha\beta}(r)$ is equal to one on the support of $\langle f_{\alpha\beta}\rangle$ and zero otherwise. Next, we observe that

$$\left\langle \frac{\delta x_\gamma}{\delta\left[\sum_{\alpha,\beta\in\Gamma}\beta\psi_{\alpha\beta}\right]}\right\rangle = \left\langle \frac{1}{M^2}\sum_{\alpha,\beta\in\Gamma}\frac{\delta x_\gamma}{\delta\beta\psi_{\alpha\beta}}\right\rangle = -4\pi r^2 g_0(r)\frac{1}{M^2}\sum_{\alpha,\beta\in\Gamma} m_{\alpha\beta}(r)e^{\beta\epsilon_{\alpha\beta}}\frac{\partial x_\gamma}{\partial\Delta_{\alpha\beta}}, \tag{45}$$

where M is the total number of sites per particle and in the last equality, we used the chain rule. So, we obtain

$$g(r) = g_0(r)\left[1 + \frac{1}{M^2\rho}\sum_{\alpha,\beta,\gamma\in\Gamma}\left(1 - \frac{2}{x_\gamma}\right)\frac{\partial x_\gamma}{\partial\Delta_{\alpha\beta}} m_{\alpha\beta}(r)e^{\beta\epsilon_{\alpha\beta}}\right], \tag{46}$$

where the terms $\frac{\partial x_\gamma}{\partial\Delta_{\alpha\beta}}$ can be determined from the law of mass action, Equation (5). In particular, using the symmetry

Downloaded by [Giorgio Pastore] at 13:57 09 July 2015

$\Delta_{\alpha\beta} = \Delta_{\beta\alpha}$, it follows

$$\frac{1}{\rho}\sum_{\gamma\in\Gamma}\left(1-\frac{2}{x_\gamma}\right)\frac{\partial x_\gamma}{\partial\Delta_{\alpha\beta}} = x_\alpha x_\beta. \tag{47}$$

From Equation (46), we can extract the contact value for the radial distribution function

$$g(\sigma^+) = g_0(\sigma^+) \times\left[1+\frac{1}{M^2\rho}\sum_{\alpha,\beta,\gamma\in\Gamma}\left(1-\frac{2}{x_\gamma}\right)\frac{\partial x_\gamma}{\partial\Delta_{\alpha\beta}}m_{\alpha\beta}(\sigma)e^{\beta\epsilon_{\alpha\beta}}\right], \tag{48}$$

where $m_{\alpha\beta}(\sigma)$ is the product of the two solid angle fractions for the $\alpha\beta$ bond when two particles are located at relative centre-to-centre distance σ. For example, for the Kern and Frenkel pair-potential [39], we would have $m_{\alpha\beta} = \chi_\alpha\chi_\beta$ with χ_{patch} the patch surface coverage. In the Bianchi *et al.* case [4] of Section 4.1, we have instead $m_{\alpha\alpha}(\sigma) = (d/\sigma)^3/3$, from Equation (29). For $g_0(\sigma^+)$, we can use the analytic solution to the Percus–Yevick approximation for the HS fluid [34], namely

$$g_0(\sigma^+) = (1+\eta/2)/(1-\eta)^2. \tag{49}$$

Next, we observe that, since $\rho g(r)4\pi r^2 dr$ gives the number of particles in the spherical shell $[r, r+dr]$ around a particle fixed on the origin, the coordination number can be estimated as follows:

$$C_n = \rho\int_\sigma^{\sigma+d} 4\pi r^2 g_0(r) \times\left[1+\frac{1}{M^2\rho}\sum_{\alpha,\beta,\gamma\in\Gamma}\left(1-\frac{2}{x_\gamma}\right)\frac{\partial x_\gamma}{\partial\Delta_{\alpha\beta}}m_{\alpha\beta}(r)e^{\beta\epsilon_{\alpha\beta}}\right]dr, \tag{50}$$

where $d = \min\{d_{\alpha\beta}\}$. The mean number of bonds per particle (the valence), $v_T = \sum_{\alpha\in\Gamma}(1-x_\alpha)$, can be also estimated from the structure as follows:

$$v_S = C_n - \lim_{T\to\infty} C_n = \frac{1}{M^2}\sum_{\alpha,\beta,\gamma\in\Gamma}\left(1-\frac{2}{x_\gamma}\right)\frac{\partial x_\gamma}{\partial\Delta_{\alpha\beta}}\Delta_{\alpha\beta}. \tag{51}$$

Then, using Equation (47) we immediately find

$$v_S = \frac{\rho}{M^2}\sum_{\alpha,\beta\in\Gamma} x_\alpha x_\beta\Delta_{\alpha\beta} = \frac{1}{M^2}\sum_{\alpha\in\Gamma}(1-x_\alpha), \tag{52}$$

where the last equality follows from the law of mass action, Equation (5). The sought for consistency between the valence calculated from the thermodynamics and the valence calculated from the structure only holds in the single site per particle case, $M = 1$.

For example, for M identical sites, we find $v_T = M(1-x)$ and, choosing Kern–Frenkel patches for which d represents the width of the attractive SW of each patch and χ the patch surface coverage, from Equation (47) follows

$$C_n = \rho\int_\sigma^{\sigma+d} 4\pi r^2 g_0(r)\left[1+x^2\chi^2 e^{\beta\epsilon}\right]dr. \tag{53}$$

7. The structure factor

We then determined the structure factor $S(k) = 1+\rho\hat{h}(k)$ with $h(r) = g(r)-1$ the total correlation function and the hat denotes the Fourier transform.

7.1. *Identical sites*

For the case of Bianchi *et al.* of Section 4.1, we find

$$S(k) = 1+4\pi\rho\int_0^\infty\left\{g_0(r)\left[1+x^2 m(r)e^{\beta\epsilon}\right]-1\right\}\times\frac{\sin(kr)}{k}r\,dr, \tag{54}$$

where x is given by Equation (7) and $m(r)$ is given by Equation (29). Choosing for $g_0(r) = \Theta(r-\sigma)$, the one obtained from the zero density limit of the HS fluid, we find the 'triangular' approximation result of Equation (A1) of Appendix. From this result follows immediately

$$\lim_{k\to 0} S(k) = 1 + 20\eta\Big[\left(e^{\beta\epsilon}-8M\eta(e^{\beta\epsilon}-1)\right)(15d^4+4d^5) - 4\left(5+\sqrt{5}\sqrt{5+4d^4M\eta(e^{\beta\epsilon}-1)(15+4d)}\right)\Big]\Big/\left(5+\sqrt{5}\sqrt{5+4d^4M\eta(e^{\beta\epsilon}-1)(15+4d)}\right)^2. \tag{55}$$

Moreover, we find

$$\lim_{T\to 0} S(0) = 1-8\eta+\frac{1}{M}, \tag{56}$$

$$\lim_{T\to\infty} S(0) = 1-8\eta+\left(3d^4+\frac{4}{5}d^5\right)\eta, \tag{57}$$

whereas for the structure factor of the reference system, we have $S_0(0) = 1-8\eta$.

In Figure 9, we show the structure factor of Equation (A1) for $M = 4$ and $T^* = 0.1$, $\eta = 0.1$.

A comparison with the simulation results of Sciortino *et al.* [4] (see their Figure 13) at $M = 2$ and $T^* = 0.055$ shows that approximation (55) breaks-down at high densities. This is shown in Figure 10 where the data of Sciortino

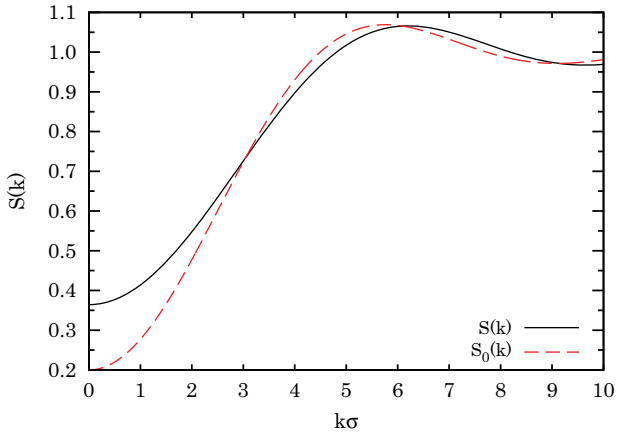

Figure 9. Structure factor for $M = 4$ and $T^* = 0.1$, $\eta = 0.1$ in the Bianchi *et al.* case using for the radial distribution function of the reference system, g_0, the zero density limit of the hard-sphere fluid. Also shown, for comparison, is the structure factor of the reference system, $S_0(k) = 1 + 24\eta(k\cos(k) - \sin(k))/k^3$.

et al. simulations are compared with the isothermal compressibility sum rule,

$$S(0) = \left[\frac{\partial}{\partial\rho}\left(\rho^2\frac{\partial\beta a}{\partial\rho}\right)\right]^{-1}, \tag{58}$$

and the relationship between the activity $\Lambda^{-3}e^{\beta\mu}$ and the density is obtained through Equation (16). We think that the fact that the structure as determined by the Equation (54) does not satisfy the isothermal compressibility sum rule of Equation (58) is a thermodynamical inconsistency not universally recognised for the Wertheim theory. In order to find accurate results for the structure, one needs to solve the

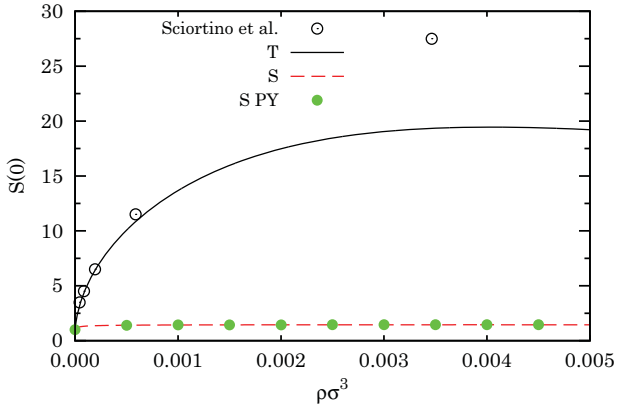

Figure 10. Structure factor at zero wave-number as a function of density for $M = 2$ and $T^* = 0.055$ in the Sciortino *et al.* simulations of Ref. [4], from the thermodynamic route (T) of the isothermal compressibility of Equation (58), from the structure route (S) of Equation (55), and from the zero wave-number limit of Equation (54) taking as a reference system the Percus–Yevick analytic solution for hard-spheres (S PY).

Wertheim Ornstein–Zernike equation with an appropriate closure [53].

8. Conclusions

We have critically analysed some recent applications of the Wertheim perturbation theory to classes of associating fluids of with non-standard phase diagrams and increasing complexity which can be today engineered in the laboratory [1]. In particular, we have illustrated the strong structural stability of the theory, which allows to get a first correct qualitative understanding of the resulting phase diagrams, even at the simplest level where all correlations of the reference system are neglected.

For fluids of HSs with M identical bonding sites, Bianchi *et al.* [3–5] discovered the 'empty liquid' scenario as M approaches two, i.e. in the presence of 'chains' only. The phenomenology when there are sites of two different kinds is more rich [6,7] and one can have 'junctions', responsible for a re-entrance of the liquid branch of the binodal, and 'rings' [8,9], responsible for a re-entrance also in the gas branch and the appearance of a second lower critical point.

In our detailed analysis of these results, we show that all the important conclusions on the qualitative behaviour of the phase diagrams can be derived uniquely from theoretical analytical considerations without the need of inputs from simulation results. For example, for the case of rings forming fluids we used as the partition function of an isolated ring the Treloar analytic expression for a freely jointed chain, unlike Rovigatti *et al.* [8,9] who use a fit of the MC data. This approximation makes immediately available a useful tool of analysis of complex phase diagrams even in the absence of more accurate but heavy numerical results.

Also, in the case of the more demanding condition of the presence of X-junctions we find that, when the energy gain for an X-junction formation, s, is low enough, we still observe a re-entrant liquid branch for $r < 1/2$ in the fluid, eventually with an 'R'-shaped spinodal in agreement with the study of Tavares *et al.* [31]. When s is sufficiently large, we observe gas–liquid coexistence also at $r < 1/3$ in agreement with the predictions of Ref. [44]. In these latter cases, a gas–liquid coexistence with a critical point at an extremely low density and temperature, unpredicted by the work of Tavares *et al.* [31], can be observed.

Moreover, we have discussed in detail the consistency between structural and thermodynamic description within Wertheim perturbation theory and in particular, the valence as obtained from the thermodynamics and from the structure. We can conclude that while the overall structural information underlying the first order perturbative level is not accurate, the theory provides a consistency condition on the estimate of bonded particles, which is satisfied only in the one-site case. An analytical expression for the radial distribution function and the structure factor has also been proposed.

Downloaded by [Giorgio Pastore] at 13:57 09 July 2015

Acknowledgements

We are grateful to José Maria Cantista de Castro Tavares for correspondence and helpful comments. Giorgio Pastore acknowledges financial support by PRIN-COFIN 2010–2011 (contract 2010LKE4CC).

Disclosure statement

No potential conflict of interest was reported by the authors.

Funding

PRIN-COFIN 2010–2011 (Giorgio Pastore) (contract 2010LKE4CC).

References

[1] Gi-Ra Yi, D.J. Pine, and S. Sacanna, J. Phys. Condens. Matter **25**, 193101 (2013).
[2] R. Fantoni and G. Pastore, J. Chem. Phys. **141**, 074108 (2014).
[3] E. Bianchi, J. Largo, P. Tartaglia, E. Zaccarelli, and F. Sciortino, Phys. Rev. Lett. **97**, 168301 (2006).
[4] F. Sciortino, E. Bianchi, J.F. Douglas, and P. Tartaglia, J. Chem. Phys. **126**, 194903 (2007).
[5] E. Bianchi, P. Tartaglia, E. Zaccarelli, and F. Sciortino, J. Chem. Phys. **128**, 144504 (2008).
[6] J. Russo, J.M. Tavares, P.I.C. Teixeira, M.M. Telo da Gama, and F. Sciortino, Phys. Rev. Lett. **106**, 085703 (2011).
[7] J. Russo, J.M. Tavares, P.I.C. Teixeira, M.M. Telo da Gama, and F. Sciortino, J. Chem. Phys. **135**, 034501 (2011).
[8] J.M. Tavares, L. Rovigatti, and F. Sciortino, J. Chem. Phys. **137**, 044901 (2012).
[9] L. Rovigatti, J.M. Tavares, and F. Sciortino, Phys. Rev. Lett. **111**, 168302 (2013).
[10] J.K. Lee, J.A. Barker, and F.F. Abraham, J. Chem. Phys. **58**, 3166 (1973).
[11] W. Ebeling and M. Grigo, Am. Phys. **37**, 21 (1980).
[12] M.J. Gillan, Mol. Phys. **49**, 421 (1983).
[13] J.-M. Caillol and J.-J. Weis, J. Chem. Phys. **102**, 7610 (1995).
[14] M.E. Fisher and Y. Levin, Phys. Rev. Lett. **71**, 3826 (1993).
[15] H.L. Friedman and G. Larsen, J. Chem. Phys. **70**, 92 (1979).
[16] M.S. Wertheim, J. Stat. Phys. **35**, 19 (1984).
[17] M.S. Wertheim, J. Stat. Phys. **35**, 35 (1984).
[18] M.S. Wertheim, J. Stat. Phys. **42**, 459 (1986).
[19] M.S. Wertheim, J. Stat. Phys. **42**, 477 (1986).
[20] N. Bjerrum, Kgl. Dan. Vidensk. Selsk. Mat.-Fys. Medd. **7**, 1 (1926).
[21] A. Tani and D. Henderson, J. Chem. Phys. **79**, 2390 (1983).
[22] R. Fantoni, A. Giacometti, F. Sciortino, and G. Pastore, Soft Matter **7**, 2419 (2011).
[23] R. Fantoni, Eur. Phys. J. B **85**, 108 (2012).
[24] R. Fantoni, *The Janus Fluid: A Theoretical Perspective* (SpringerBriefs in Physics) (Springer, New York, 2013).
[25] R. Fantoni and G. Pastore, Europhys. Lett. **101**, 46003 (2013).
[26] R. Fantoni and G. Pastore, Phys. Rev. E **87**, 052303 (2013).
[27] E. Bianchi, R. Blaak, and C. N. Likos, Phys. Chem. Chem. Phys. **13**, 6397 (2011).
[28] B.D. Marshall, D. Ballal, and W.G. Chapman, J. Chem. Phys. **137**, 104909 (2012).
[29] B.D. Marshall and W.G. Chapman, J. Chem. Phys. **138**, 044901 (2013).
[30] B.D. Marshall and W.G. Chapman, Phys. Rev. E **87**, 052307 (2013).
[31] J.M. Tavares and P.I. Teixeira, J. Phys. Condens. Matter **24**, 284108 (2012).
[32] G. Jackson, W.G. Chapman, and K.E. Gubbins, Mol. Phys. **65**, 1 (1988).
[33] N.F. Carnahan and K.E. Starling, J. Chem. Phys. **51**, 635 (1969).
[34] J.-P. Hansen and I.R. McDonald, *Theory of Simple Liquids*, 3rd ed. (Academic Press, London, 2005).
[35] H. Liu, S.K. Kumar, F. Sciortino, and G.T. Evans, J. Chem. Phys. **130**, 044902 (2009).
[36] L. Vega, E. de Miguel, L.F. Rull, G. Jackson, and I.A. McLure, J. Chem. Phys. **96**, 2296 (1992).
[37] H. Liu, S. Garde, and S. Kumar, J. Chem. Phys. **123**, 174505 (2005).
[38] G. Malescio, G. Franzese, G. Pellicane, A. Skibinsky, S.V. Buldyrev, and H.E. Stanley, J. Phys. Condens. Matter **14**, 2193 (2002).
[39] N. Kern and D. Frenkel, J. Chem. Phys. **118**, 9882 (2003).
[40] R. Fantoni, D. Gazzillo, A. Giacometti, M.A. Miller, and G. Pastore, J. Chem. Phys. **127**, 234507 (2007).
[41] D. de las Heras, J.M. Tavares, and M.M. Telo da Gama, J. Chem. Phys. **134**, 104904 (2011).
[42] D. de las Heras, J.M. Tavares, and M.M. Telo da Gama, Soft Matter **7**, 5615 (2011).
[43] J.M. Tavares, P.I.C. Teixeira, and M.M. Telo de Gama, Phys. Rev. E **80**, 021506 (2009).
[44] J.M. Tavares, P.I.C. Teixeira, M.M. Telo da Gama, and F. Sciortino, J. Chem. Phys. **132**, 234502 (2010).
[45] R.P. Sear and G. Jackson, Phys. Rev. E **50**, 386 (1994).
[46] A. Galindo, S. Burton, G. Jackson, D. Visco, and D.A. Kofke, Mol. Phys. **100**, 2241 (2002).
[47] A. Avlund, G. Kontogeorgis, and W. Chapman, Mol. Phys. **109**, 1759 (2011).
[48] T. Tlusty and S.A. Safran, Science **290**, 1328 (2000).
[49] F. Sciortino, A. Giacometti, and G. Pastore, Phys. Rev. Lett. **103**, 237801 (2009).
[50] P.J. Flory, *Statistical Mechanics of Chain Molecules* (Interscience Publishers, New York, 1969), Chap. VIII, Section 3.
[51] E. Fermi, *Termodinamica* (Bollati Boringhieri, Torino, 1958), §18.
[52] F. Smallenburg and F. Sciortino, Nature Phys. **9**, 554 (2013).
[53] J. Chang and S.I. Sandler, J. Chem. Phys. **102**, 437 (1995).

Appendix. The structure factor in the 'triangular' approximation

Choosing $g_0(r) = \Theta(r - \sigma)$ in Equation (54) with $m(r)$ defined as in Equation (29), we find

$$\begin{aligned} S(k) = 1 + 80\eta\Big[&(15k^3 - 90d^4k^3M\eta - 24d^5k^3M\eta)\cos(k) \\ &+ (90d^4k^3M\eta + 24d^5k^3M\eta + 10d^3k^3)e^{\beta\epsilon}\cos(k) \\ &+ 3\sqrt{5}k^3\sqrt{5 + 4d^4M\eta(e^{\beta\epsilon} - 1)(15 + 4d)}\cos(k) \\ &+ (-15k^2 + 90d^4k^2M\eta + 24d^5k^2M\eta)\sin(k) \\ &+ (-90d^4k^2M\eta - 24d^5k^2M\eta)e^{\beta\epsilon}\sin(k) \end{aligned}$$

Downloaded by [Giorgio Pastore] at 13:57 09 July 2015

$$+(15d^2k^2+30)e^{\beta\epsilon}\sin(k)$$
$$+\ -3\sqrt{5}k^2\sqrt{5+4d^4M\eta(e^{\beta\epsilon}-1)(15+4d)}\sin(k)$$
$$+30(dk\cos(k(1+d))-\sin(k(1+d)))e^{\beta\epsilon}\Big]\Big/$$
$$\left[k^5\left(5+\sqrt{5}\sqrt{5+4d^4M\eta(e^{\beta\epsilon}-1)(15+4d)}\right)^2\right]. \tag{A1}$$

From this expression, one immediately sees that the high-temperature limit, $\beta \to 0$, of the structure factor is independent from the number of sites, M.

Downloaded by [Giorgio Pastore] at 13:57 09 July 2015